Aqueous Synthesis of Mixed Yttrium−Barium Oxalates

Nathalie Jongen, Jacques Lemaître,* Paul Bowen, and Heinrich Hofmann

Powder Technology Laboratory, Materials Science and Engineering Department, EPFL, CH-1015 Lausanne, Switzerland

Received August 25, 1998. Revised Manuscript Received January 11, 1999

The experimental domain for seeded precipitation of mixed (Y, Ba) oxalates has been investigated in the system $[Y(OH)_3, Ba(OH)_2]-H_2C_2O_4-[HNO_3, NaOH)]-H_2O$. A statistically designed series of experiments was performed in order to highlight the relative effects of various factors on the precipitate composition: reaction temperature (30−40 °C), rate of coreactant addition, volume of added seeding suspension, and aging time of the precipitate. The recently discovered $Y_2Ba_4(C_2O_4)_7 \cdot 18H_2O$ oxalate, in the form of octahedral crystals, has been detected in all the precipitates, together with another unknown mixed (Y, Ba) oxalate. Calculations based on elemental composition and thermogravimetric data, assuming residual amounts of $BaC_2O_4 \cdot 0.5H_2O$, allowed the estimation of the probable stoichiometric formula of this new compound: $Y_2Ba_2(C_2O_4)_5 \cdot wH_2O$. From SEM observations this compound precipitates in the form of pinacoidal crystals. The results of the statistical analysis have shown that the formation of $Y_2Ba_4(C_2O_4)_7 \cdot 18H_2O$ is favored by lower temperature, higher reactant addition rate, and lower volume of seeding suspension. The formation of $Y_2Ba_2(C_2O_4)_5 \cdot wH_2O$ occurs more readily at higher temperatures, for slower reactant addition. The two mixed (Y, Ba) oxalates and $BaC_2O_4 \cdot 0.5H_2O$ crystals were already present in the seeding suspension. Therefore, the seed suspension could not improve the selective formation of any mixed oxalate in the seeded, fed-batch system used. The most favorable experimental conditions were then successfully transferred to a new segmented flow tubular reactor, recently developed in our laboratory, allowing the selective precipitation of $Y_2Ba_4(C_2O_4)_7 \cdot 18H_2O$ for the first time.

Introduction

One of the main routes for the elaboration of good quality mixed oxides is via the coprecipitation of the powder precursors.[1−12] In the field of high-temperature superconducting oxides, oxalate coprecipitation followed by a firing at a suitable temperature was first mentioned by Bednorz and Müller[9] for the La−Ba−Cu−O superconductors. Other mixed oxide systems (barium titanate, yttrium doped ceria, neodynium doped barium cerium oxides) have also been successfully produced using oxalate coprecipitation.[13−15] A tool for the calculation of solubility isotherms of the individual metal oxalates has been previously developed for the system $[Y(OH)_3, Ba(OH)_2\ Cu(OH)_2]-H_2C_2O_4-[HNO_3, NaOH)]-H_2O$.[10] The ternary coprecipitation (Y, Ba, Cu) has been experimentally studied using this tool as a starting point, and results showed the existence of several mixed oxalates unaccounted for in the solid phases used in the model.[11] One of the mixed oxalates was $BaCu(C_2O_4)_2 \cdot 6H_2O$ discovered and characterized by Hallock et al.[12] Other authors have also mentioned the existence of mixed oxalates in their ternary studies on Y, Ba, Cu oxalates and others (yttrium-doped ceria), but little further investigation in order to identify these mixed oxalates has been performed.[6,7,13,16] Another of the mixed oxalates has been identified as $Y_2Ba_4(C_2O_4)_7 \cdot zH_2O$,[17] although it was not possible to isolate it as an entirely pure phase.

In the present study, the experimental conditions around the nearly selective precipitation of the $Y_2Ba_4(C_2O_4)_7 \cdot zH_2O$ mixed oxalate[17] were investigated using

* To whom correspondence should be sent.

(1) Morgan, D.; Maric, M.; Luss, D.; Richardson, J. T. *J. Am. Ceram. Soc.* **1990**, *73*, 3557.
(2) Kim, D.-J.; Kroeger, D. M. *J. Mater. Sci.* **1993**, *28*, 4744.
(3) Dasgupta, M.; Dixit, S. G. *Jpn. J. Appl. Phys.* **1992**, *31*, 35.
(4) Wang, X.-Z.; Baüerle, D.; Oberreiter, M.; Gritzner, G. *High-Temp. Supercond. Proc. ICMC'90 Top−Conf. Mater. Aspects High-Temp. Supercond.* 1990, p 347.
(5) Das Sharma, A.; Basu, R. N.; Maiti, H. S. *J. Mater. Sci. Lett.* **1992**, *11*, 122.
(6) Bhargava, A.; MacKinnon, I. D. R.; Yamashita, T.; Page, T. *Physica C* **1995**, *241*, 53.
(7) Terryll, K.; Rao, K. V.; Wang, N. L.; Zakharchenko, I. V.; Muhammed, M.; Balachadran, U. *Supercond. Sci. Technol.* **1995**, *8*, 296.
(8) Wang, L.; Zhang, Y.; Muhammed, M. *J. Mater. Chem.* **1995**, *5*, 309.
(9) Bednorz, J. G.; Müller, K. A. *Zeitschrift für Physik B* **1986**, *64*, 189.
(10) Rubattel, S.; Lemaître, J.; Bowen, P.; Ring, T. A. *J. Cryst. Growth* **1994**, *135*, 135.
(11) Rubattel, S. EPFL, Thesis No. 1160, Lausanne, Switzerland, 1993.
(12) Hallock, R. B.; Rhine, W. E.; Cima, M. J.; Bott, S. G.; Atwood, J. L. *Ceram. Trans.* **1990**, *13*, 251.
(13) Van Herle, J.; Horita, T.; Kawada, T.; Sakai, N.; Yokokawa, H.; Dokiya, M. *J. Am. Ceram. Soc.* **1997**, *80*, 933.
(14) Park, Z. H.; Shin, H. S.; Lee, B. K.; Cho, S. H. *J. Am. Ceram. Soc.* **1997**, *80*, 1599.
(15) Chen, F. L.; Wang, P.; Sørensen, O. T.; Meng, G. Y.; Peng, D. K. *J. Mater. Chem.* **1997**, *7*, 1533.
(16) Millar; G. J.; Bell, R. J.; Bhargava, A.; MacKinnon, I. D. R.; Fredericks, P. M. *Mater. Lett.* **1995**, *25*, 75.
(17) Rubattel, S.; Jongen, N.; Lemaître, J.; Bowen, P.; Merk N. *J. Mater. Sci. Lett.* **1995**, *14*, 1196.

10.1021/cm980745s CCC: $18.00
Published on Web 02/25/1999

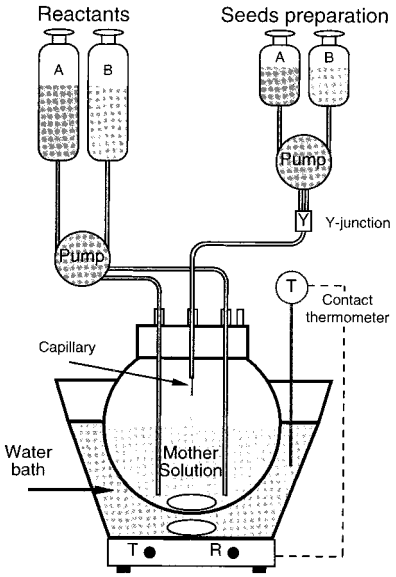

Figure 1. Schematic representation of the experimental set up used for the seeded batch experiments.

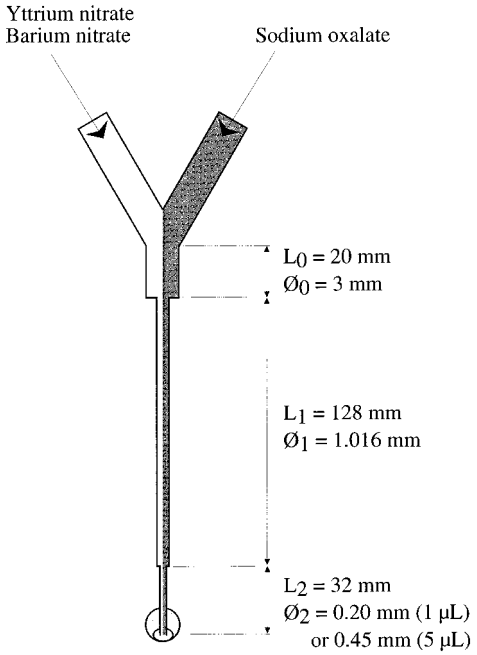

Figure 2. Description of the mixing unit used to prepare the seeding suspension.

a statistical experimental design, with the aim of improving the selectivity of the reaction. A seeded, fed-batch reactor was used for the initial statistical experimental design, and these results were transferred to a segmented flow tubular reactor recently developed in our laboratory[20,21] with the aim of producing the pure $Y_2Ba_4(C_2O_4)_7 \cdot zH_2O$ phase.

Experimental Section

1. Seeded, Fed-Batch Reactor. Sixteen precipitation experiments were performed by adding simultaneously a mixed solution of yttrium nitrate ($Y(NO_3)_3 \cdot 5H_2O$) and barium nitrate ($Ba(NO_3)_2$) (100 mL) and a sodium oxalate solution ($Na_2C_2O_4$) (100 mL) to a solution presaturated with the same salts (mother solution, 2 L) contained in a batch reactor preheated at the desired temperature. The experimental set up is depicted in Figure 1. Constant agitation was maintained during the experiments (magnetic stirrer, 500 rpm). Each experiment was started by adding a given volume of seed solution (10 or 20 mL); the seed suspension was obtained by flowing simultaneously equivalent volumes of the nitrate and oxalate solutions through a mixing unit, described in detail hereafter. The seed solution was added dropwise to the mother solution at the same flow rate as, and in addition to, the main reacting solutions. The mother solution contained 4.81×10^{-6} mol/L of yttrium nitrate, 3.55×10^{-3} M of barium nitrate, and 1.40×10^{-3} M of sodium oxalate; its pH was 5.7. The compositions of the reactant solutions were 0.0274 M yttrium nitrate and 0.0548 M barium nitrate (solution A), and 0.0892 M sodium oxalate (solution B). The reactants were added simultaneously at a constant flow rate (75 or 100 mL/h for each reactant) to the mother solution, through separate nozzles, the outlet of which was kept in the vicinity of the stirring bar. After reactant addition, the solution was aged for a prescribed time. After aging, the suspensions were left to sediment for 1 h at ambient temperature and filtered through a 0.2 μm cellulose membrane. The precipitates were washed three times with their volume of ethanol and dried over silica gel in a desiccator until constant weight was obtained. The powders obtained were loosely agglomerated and colorless.

The powder referred to as "seeds" was prepared by flowing 100 mL of solution A to the same volume of solution B through the mixing unit mentioned above at a rate of 75 mL/h for each reactant; the so obtained suspension was filtered immediately through a 0.2 μm cellulose membrane and subsequently treated in the same way as the other powders.

The mixing unit, schematized in Figure 2, consists of three parts. The two reactant solutions join at a Y junction, then they go through a tube with a narrower section before entering a glass capillary with a 3.2 cm length and 0.20 or 0.45 mm diameter (volume, 1 or 5 μL, respectively). The results of measurements and calculations made for four different cases (applied flow rate, 2×75 or 2×100 mL/h; capillary volume, 1 or 5 μL) are presented in Table 1. The mean lifetime and the volume of a droplet were measured. The real flow rates were calculated; they vary from 150.2 to 180.4 mL/h. The residence time in the mixer was also calculated and is between 5.0 and 5.9 s. From a calculation of the Reynolds numbers for each case, the flow is laminar in each part of the mixer. The maximum Reynolds number encountered is 295 for the small capillary volume and the large flow rate. The velocities in parts L_0 and L_1 are not significantly different according to conditions, whereas the velocity in the capillary varies greatly according to the capillary volume, from 134 to 148 cm/s for the 1 μL capillary to 28−32 cm/s for the 5 μL capillary.

The 16 experiments performed in the batch reactor were organized in a multifactorial experimental design (2^4 factorial design), four factors being applied at two levels each. The factors are (A) seed suspension volume, (B) reactant addition rate, (C) aging time, and (D) reaction temperature. The definitions and levels of the factors are reported in Table 2. For the sake of convenience, the full design was split in two blocks, and the effect (X) was confounded with the third-order interaction ABCD.[18] The results were analyzed using the ANOVA technique.[18]

2. Segmented Flow Tubular Reactor. This precipitation experiment was performed by using our new segmented flow tubular reactor described elsewhere.[20,21] The experiment was carried out by mixing a 1.28×10^{-3} M yttrium nitrate and 5.99×10^{-3} M barium nitrate solution (250 mL) with a 4.66×10^{-3} M sodium oxalate solution (250 mL) in the mixer−segmenter. The reactants were mixed at a constant flow rate

(18) Montgomery, D. C. *Design and Analysis of Experiments*; John Wiley & Sons: New York, 1991.
(19) Dollimore, D.; Fletcher, A. *Proceedings of the 2nd European Symposium on Thermal Analysis*, September 1−4, 1981, 289.
(20) Jongen, N.; Lemaître, J.; Bowen, P.; Hofmann, H. *Proceedings of the 5th World Congress of Chemical Engineering*; San Diego, California, July 14−18, 1996, 5, p 31.
(21) Vacassy, R.; Jongen, N.; Lemaître, J.; Bowen, P.; Hofmann H. *Proceedings of the 3rd International Particle Technology Forum*, Brighton, United Kingdom, July 6−9, 1998.

Table 1. Mixing Unit: Measured and Calculated Parameters

applied flow rate	2 × 75 mL/h		2 × 100 mL/h	
capillary volume (μL)	1	5	1	5
mean volume of a droplet (mL)	1.7×10^{-2}	1.8×10^{-2}	1.9×10^{-2}	2.1×10^{-2}
mean time of existence of a droplet (s)	0.41	0.42	0.32	0.33
real flow rate (mL/h)	150.2	159.4	166.3	180.4
residence time (s)	5.9	5.7	5.3	5.0
Reynolds number in L_0	18	19	20	21
Reynolds number in L_1	52	55	58	63
Reynolds number in capillary	266	126	295	143
speed in L_0 (cm/s)	0.5	0.6	0.7	0.7
speed in L_1 (cm/s)	5.2	5.4	5.7	6.2
speed in capillary (cm/s)	134	28	148	32

Table 2. Experimental Design: Factor Definitions and Experimental Array

factors	definition	low level	high level
A	seed suspension volume	2 × 5.0 mL	2 × 10.0 mL
B	addition rate (mL/h)	75	100
C	ageing time (h)	2.0 h	3.0 h
D	temperature (°C)	30	40
X=ABCD	block	I	II
	capillary volume (μL)	≡1	≡5

2^4 design		factors				
sample	treatment	seed volume (mL)	addition rate (mL/h)	ageing time (h)	temp (°C)	block
1	(X)	2 × 5	75	2	30	II
2	A	2 × 10	75	2	30	I
3	B	2 × 5	100	2	30	I
4	AB(X)	2 × 10	100	2	30	II
5	C	2 × 5	75	3	30	I
6	AC(X)	2 × 10	75	3	30	II
7	BC(X)	2 × 5	100	3	30	II
8	ABC	2 × 10	100	3	30	I
9	D	2 × 5	75	2	40	I
10	AD(X)	2 × 10	75	2	40	II
11	BD(X)	2 × 5	100	2	40	II
12	ABD	2 × 10	100	2	40	I
13	CD(X)	2 × 5	75	3	40	II
14	ACD	2 × 10	75	3	40	I
15	BCD	2 × 5	100	3	40	I
16	ABCD(X)	2 × 10	100	3	40	II

(72 mL/h per reactant solution). The solutions and the whole reactor were maintained at 25 °C in a water bath. After the mixing step, the precipitating suspension had a residence time of 15 min in the tubular reactor and was then collected and stored at 3 °C to slow any possible further reaction. At the end of the experiment, the suspension was centrifuged at 4000 rpm for 15 min. The filtrate was separated, filtered using a 0.2 μm membrane, and treated for chemical analysis. The powder is alternatively washed with 2-propanol and centrifuged three times and finally filtered using a 0.2 μm membrane. The powder was dried over silica gel in a desiccator until constant weight was obtained. Longer residence times in the tubular reactor, e.g. 60 min, yielded no marked changes in the precipitate properties.

3. Characterization Methods. XRD measurements were made using a Siemens D500 diffractometer, with the Ni-filtered Cu Kα radiation. The powders were observed in the SEM mode on a JEOL model JSM-6300F electron microscope; the chemical composition of individual crystals was investigated by dispersive energy spectroscopy in a Cambridge S-360 microscope, equipped with the Tracor "Voyager" acquisition system. Thermogravimetric analysis (TGA) was performed under dry air (200 mL/min) in a Mettler TG4000 thermobalance (heating rate 10 °C/min). Before starting TGA experiments, the samples were maintained at 25 °C under dry air flow until constant weight was achieved. A preliminary set of experiments was performed in order to locate the weight losses accurately (30−1000 °C without dwell). Thereafter, the gravimetric losses were measured accurately after a 60-min dwell at each characteristic temperature, determined from a minimum of the derivative of the weight loss curve. The yttrium and barium contents of the precipitates and filtrates were analyzed by atomic emission spectroscopy (ICP-AES, Perkin-Elmer, Plasma 2000 software). The oxalate content in the filtrates was determined using Total Organic Carbon analysis (Shimadzu TOC 5000).

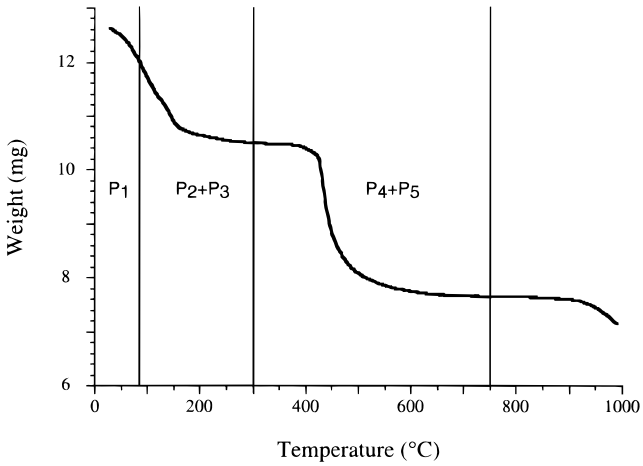

Figure 3. Thermal decomposition of sample 15, heating rate 10 °C/min.

Results and Discussion

Seeded Batch Reactor. All the powders are assumed to be composed of three phases: the mixed oxalate $Y_2Ba_4(C_2O_4)_7 \cdot 18H_2O$,[14] a new mixed oxalate with the presumed formula $Y_2Ba_x(C_2O_4)_{x+3} \cdot wH_2O$, and the barium oxalate $BaC_2O_4 \cdot 0.5H_2O$.

Characterization of the Precipitates. A typical thermogram is presented in Figure 3 without the dwell periods. All the powders, including the seed powder, exhibit the same thermal decomposition steps: A first weight loss, corresponding to the dehydration of the phase $Y_2Ba_4(C_2O_4)_7 \cdot 18H_2O$,[17] occurs between 30 and 90 °C (loss P_1); a second loss, ascribed to the dehydration of the new phase $Y_2Ba_x(C_2O_4)_{x+3} \cdot wH_2O$, occurs between 90 and 150 °C (P_2); a third loss, attributed to the dehydration of $BaC_2O_4 \cdot 0.5H_2O$,[19] occurs between 150 and 300 °C (P_3); a fourth loss, corresponding to the simultaneous decomposition of $Y_2Ba_4(C_2O_4)_7$ and $Y_2Ba_x(C_2O_4)_{x+3}$ into Y_2O_3 and $BaCO_3$, is observed between 300 and 450 °C (P_4); a fifth loss corresponding to the decomposition of barium oxalate into carbonate [11] occurs in the range 450−750 °C; finally, barium carbonate starts decomposing at 900 °C, but this process was not completed by the end of the measurements. The weight losses calculated from the gravimetric experiments are summarized in Table 3, together with the ratios $P_1/(P_2 + P_3)$. The limits of the temperature ranges for gravimetric analysis were selected as the most probable

Table 3. Experimental Results

sample	gravimetric losses P_1[a] (%)	$P_2 + P_3$[b] (%)	$P_4 + P_5$[c] (%)	weight loss ratio: $P_1/(P_2 + P_3)$	XRD intensity ratio: (I_1/I_2)	atomic ratio: Ba/Y
1	6.3	8.9	22.6	0.71	0.61	1.63
2	7.0	7.9	22.0	0.89	1.01	1.74
3	8.1	6.2	22.5	1.30	1.26	1.71
4	6.0	9.0	22.8	0.66	0.57	1.61
5	7.0	8.6	22.7	0.81	0.69	1.68
6	3.2	11.5	23.4	0.28	0.08	1.41
7	3.8	11.1	23.3	0.34	0.17	1.45
8	7.9	7.1	21.6	1.11	1.35	1.77
9	5.5	8.8	22.5	0.63	0.65	1.55
10	3.6	11.2	23.4	0.32	0.16	1.47
11	3.5	11.3	23.5	0.31	0.12	1.45
12	6.2	8.8	23.9	0.70	0.62	1.62
13	4.3	10.6	23.0	0.41	0.26	1.51
14	6.4	9.0	22.6	0.72	0.59	1.57
15	7.6	6.3	22.7	1.21	1.19	1.63
16	6.5	8.8	22.4	0.74	0.60	1.62
"seeds"	11.3	6.1	22.3	1.85		1.34

[a] Measured from 30 to 90 °C [b] Measured from 90 to 300 °C. [c] Measured from 300 to 750 °C.

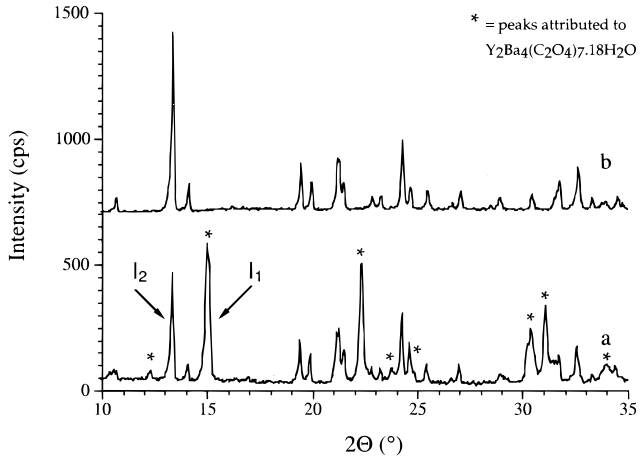

Figure 4. (a) XRD pattern of (a) powder 15 and (b) powder 15 heated at 90 °C.

minimum valleys between the TGA peaks; the intensities of unresolved peaks, such as P_2 and P_3, or P_4 and P_5 were grouped for the computations. The gravimetric losses reported in Table 3 were little sensitive to slight changes in boundary temperatures.

All the powders investigated presented similar XRD patterns, although the relative intensities of some reflections varied from sample to sample. A typical XRD pattern (sample 15) is presented in Figure 4a. Barium oxalate ($BaC_2O_4 \cdot 0.5H_2O$) cannot be detected on any of the diffractograms, whereas the characteristic lines of the mixed oxalate $Y_2Ba_4(C_2O_4)_7 \cdot 18H_2O$[17] are always present. The reflection at 14.95° 2θ (I_1) corresponds to the already known phase $Y_2Ba_4(C_2O_4)_7.zH_2O$, whereas the reflection at 13.36° 2θ (I_2) presumably corresponds to be the main peak of phase $Y_2Ba_x(C_2O_4)_{x+3} \cdot wH_2O$. The intensity ratios ($I_1/I_2$) (Table 3) indicate that the weight loss ratio $P_1/(P_2 + P_3)$ is correlated to the XRD intensity ratio variation (I_1/I_2). In fact, when the XRD intensity ratio increases, the corresponding weight loss also increases, indicating that the amount of the $Y_2Ba_x(C_2O_4)_{x+3} \cdot wH_2O$ phase in the precipitate varies according to experimental conditions. Figure 4b depicts the XRD pattern of sample 15 after thermal treatment at 90 °C: A series of peaks has disappeared, all of which can be attributed to $Y_2Ba_4(C_2O_4)_7 \cdot 18H_2O$, indicating that this phase has decomposed into an amorphous

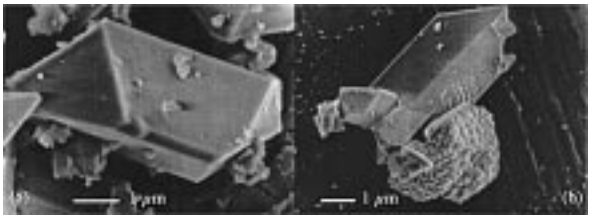

Figure 5. SEM micrographs: (a) powder 12 showing a mixed yttrium−barium oxalate pinacoidal crystal; (b) powder 15 heated at 90 °C, showing pinacoidal crystals and a decomposed $Y_2Ba_4(C_2O_4)_7 \cdot 18H_2O$ octahedral crystal.

dehydration product; the remaining reflections can thus be ascribed to the $Y_2Ba_x(C_2O_4)_{x+z} \cdot wH_2O$ phase, which does not decompose upon heating at 90 °C.

The atomic ratios Ba/Y of the powders vary in the range 1.41−1.77 (Table 3); it can therefore be concluded that the new mixed oxalate contains less barium than $Y_2Ba_4(C_2O_4)_7 \cdot 18H_2O$.

Two different crystal morphologies were identified by SEM: octahedra, corresponding to $Y_2Ba_4(C_2O_4)_7 \cdot 18H_2O$, and unknown pinacoidal crystals. According to qualitative EDS analysis, the pinacoids contain both Y and Ba and can thus be ascribed to the new $Y_2Ba_x(C_2O_4)_{x+3} \cdot wH_2O$ compound. Figure 5a depicts powder 12, mainly composed of such pinacoids. Powder 15 was also observed after heating at 90 °C: Figure 5b shows a partial decomposition of the octahedras, whereas the pinacoids are left intact supporting our interpretation of the XRD data.

Determination of the Composition of the New Mixed Oxalate. The stoichiometry of the new $Y_2Ba_x(C_2O_4)_{x+3} \cdot wH_2O$ compound and the molar fractions of both mixed oxalates in the precipitates have been calculated as explained below, from the weight losses P_1, $(P_2 + P_3)$, and $(P_4 + P_5)$ and the atomic ratios Ba/Y. To reduce the scatter due to experimental errors, the computations have been performed with the adjusted values of P_1, $(P_2 + P_3)$, and $(P_4 + P_5)$ and Ba/Y, calculated according to the statistical analyses ($p < 0.05$).

The precipitates obtained are assumed to have the following composition:

$$a\,Y_2Ba_4(C_2O_4)_7 \cdot zH_2O + b\,Y_2Ba_x(C_2O_4)_{x+3} \cdot wH_2O + c\,BaC_2O_4 \cdot 0.5H_2O$$

Table 4. Weight Fractions of Calculated Compositions of Mixed Oxalates and Barium Oxalate for Various Conditions

	weight fractions (%)		
sample	$Y_2Ba_4(C_2O_4)_7 \cdot 18H_2O$	$Y_2Ba_2(C_2O_4)_5 \cdot 8H_2O$	$BaC_2O_4 \cdot 0.5H_2O$
1	26.31	59.49	14.21
2	37.62	52.67	9.71
3	42.34	48.83	8.83
4	31.48	56.41	12.11
5	31.71	53.90	14.38
6	15.51	73.13	11.36
7	20.48	69.01	10.50
8	36.83	50.85	12.32
9	28.87	56.14	15.00
10	12.26	73.87	13.87
11	17.52	70.79	11.69
12	33.73	52.25	14.02
13	24.26	64.27	11.48
14	33.82	50.95	15.23
15	38.81	47.97	13.21
16	29.15	60.26	10.59

a, b, and c being the molar fractions of the constituent phases ($a + b + c = 1$). Then, P_1 corresponds to the dehydration of $Y_2Ba_4(C_2O_4)_7 \cdot zH_2O$, $(P_2 + P_3)$ to the simultaneous dehydration of the two other phases, and $(P_4 + P_5)$ to the decomposition of the oxalates into Y_2O_3 and $BaCO_3$ with the evolution of CO and CO_2. The molar fraction of $Y_2Ba_x(C_2O_4)_{x+3} \cdot wH_2O$ is thus given by

$$b = (1 - a(2r - 3))/(2r - x + 1)$$

with $r = Ba/Y$.

The molar fraction of $BaC_2O_4 \cdot 0.5H_2O$ is given by

$$c = 1 - a - b$$

The following conditions were imposed: $2 < x < 4$; z, $w > 0$ and $0 < a, b, c < 1$. Values of x, z, w, and a are then calculated by successive approximations for each sample, to minimize the sum of the squares of the differences between the observed and calculated gravimetric losses P_1, $(P_2 + P_3)$, and $(P_4 + P_5)$. Averaging the results obtained from the 16 separate experiments confirms that the octahedral mixed oxalate contains 18 molecules of water of hydration and gives $Y_2Ba_2(C_2O_4)_5 \cdot 8H_2O$ as the most probable stoichiometry of the pinacoidal mixed oxalate. If the hypothesis of simple barium oxalate formation were to be rejected, another possible way to interpret the results is to ascribe variable amounts of Ba to the mixed oxalate, the stoichiometric formula of which would then read $Y_2Ba_{2+y}(C_2O_4)_{5+y} \cdot (8 + 0.5y)H_2O$, with $0.7 < y < 1.3$.

The precipitate compositions reported in Table 4 have been calculated assuming the following basic constituents: $Y_2Ba_4(C_2O_4)_7 \cdot 18H_2O$, $Y_2Ba_2(C_2O_4)_5 \cdot 8H_2O$, and $BaC_2O_4 \cdot 0.5H_2O$.

Effect of Experimental Parameters on Precipitate Composition. A detailed ANOVA analysis has been made on the XRD results (I_1/I_2) reported in Table 3 and on the weight fractions of $Y_2Ba_4(C_2O_4)_7 \cdot 18H_2O$ and $BaC_2O_4 \cdot 0.5H_2O$, reported in Table 4. A preliminary analysis of the results has shown that interaction ABCD, confounded with the main effect of the blocks, was in most cases the prevailing source of variation. Moreover, according to previous work, aging time can be assumed to play no significant role in the experimental domain investigated here. Therefore, the results will be discussed with respect to the effects associated with blocks instead of the aging time. Considering that the block effect is confounded with the capillary effect, the capillary volume will be used for the following discussion.

The experimental values of $\log(I_1/I_2)$ (Figure 6a), the weight fraction of $Y_2Ba_4(C_2O_4)_7 \cdot 18H_2O$ (Figure 6b), and the weight fraction of barium oxalate (Figure 6c) are compared to the adjusted values calculated according to the statistical models (type I error risk $p < 0.01$). Although these responses were obtained independently, the similarity of the patterns shown in parts and b of Figure 6 is striking, supporting the hypothesis used for calculating the phase composition of the precipitates. The complex aspect of the patterns shown in Figure 6 reveals that the final composition of the precipitates is determined by the intricate interplay of the experimental factors.

Figure 6b shows that the effect of temperature is more or less identical for all the experimental conditions. When the temperature increases, the quantity of $Y_2Ba_4(C_2O_4)_7 \cdot 18H_2O$ slightly decreases. A larger capillary volume reduces the mean amount of this same compound. Nevertheless, the other parameters must be discussed because of their different influence according to the capillary volume used. With a 1 μL capillary and a 150 mL/h reactant rate, a larger volume of seed suspension induces an augmentation of the $Y_2Ba_4(C_2O_4)_7 \cdot 18H_2O$ fraction. If the reactant rate is 200 mL/h, increasing the seed suspension volume will increase the amount of $Y_2Ba_4(C_2O_4)_7 \cdot 18H_2O$. Therefore, the seed suspension volume and the reactant rate interact together and their interaction also depends on the capillary volume.

Figure 6b also shows that the best conditions for improving the selective formation of $Y_2Ba_4(C_2O_4)_7 \cdot 18H_2O$ are 1 μL capillary, 30 °C, 10 mL of seed suspension, and a 200 mL/h flow rate (indicated by pale gray arrow in Figure 6b); the most advantageous conditions for the formation of the $Y_2Ba_2(C_2O_4)_5 \cdot 8H_2O$ phase correspond to a larger volume of seed solution, higher temperature, 5 μL capillary, and slower reactant addition (indicated by the dark gray arrow in Figure 6b).

According to Figure 6c, the weight fraction of $BaC_2O_4 \cdot 0.5H_2O$ in the precipitates varies only slightly (9−15%) compared to the variation of $Y_2Ba_4(C_2O_4)_7 \cdot 18H_2O$ (12−42%). Figure 6c shows the interaction of temperature with other experimental factors: At 30 °C, the use of the 5 μL capillary either increases or does not change the weight fraction of barium oxalate, whereas samples prepared with the 5 μL capillary at 40 °C always contain less barium oxalate than the corresponding samples prepared with the other capillary.

The complexity of the system is real and reflects the complex interplay of the experimental factors rather than random experimental scattering. The seeding suspension flow in the mixing unit is laminar. The mean time of existence of a droplet and the residence time in the mixer of a given volume do not significantly change according to the capillary diameter. The only difference between the two types of mixing unit is the speed, which is much larger at the exit of the 1 μL capillary ($\approx$140 cm/s) than the exit of the other (30 cm/s). The mixing conditions in the droplet might be different according

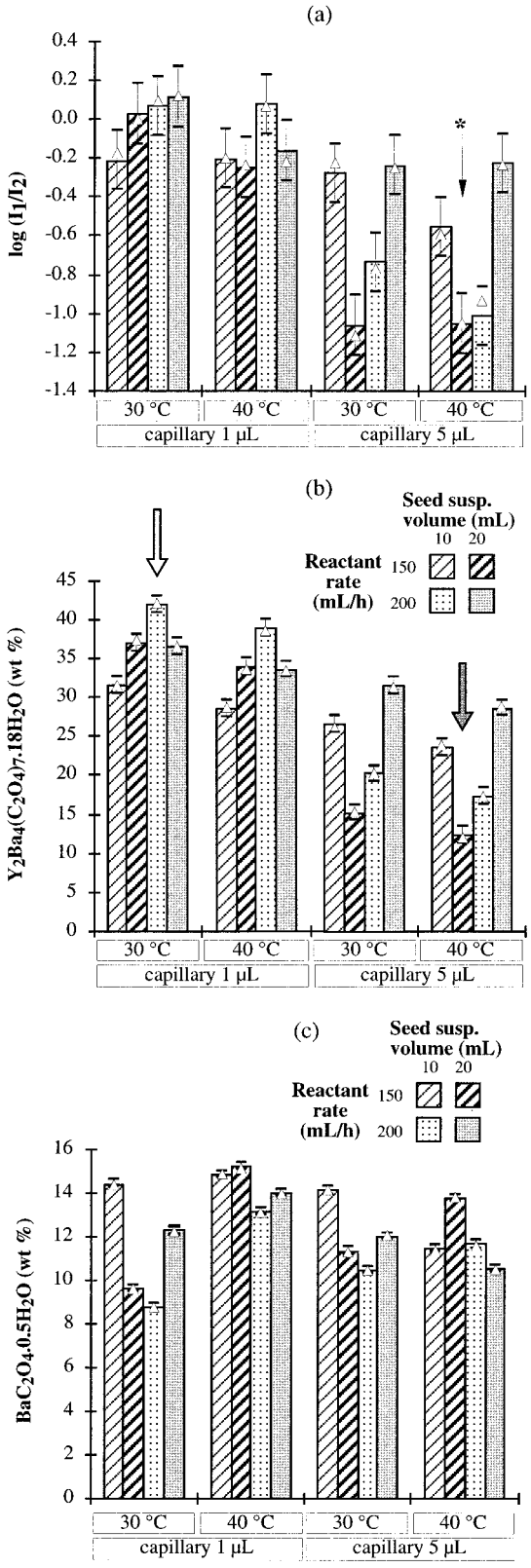

Figure 6. Statistical analysis: Δ = experimental value; bars represent adjusted value; error intervals = ±3SE. (a) $\log(I_1/I_2)$; calculated value * = −1.041 ($p < 0.01$). (b) Weight ratio $Y_2Ba_4(C_2O_4)_7{\cdot}18H_2O$ (%) ($p < 0.01$). (c) Weight ratio $BaC_2O_4{\cdot}0.5H_2O$ (%) ($p < 0.01$).

to the capillary volume as the kinetic energy dissipated in the droplet is different. This should influence the number and the type of seeds prepared in the mixing unit. If more efficient mixing conditions are ensured

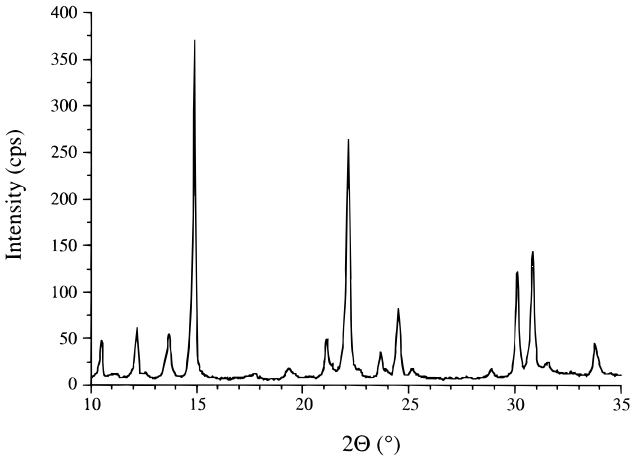

Figure 7. X-ray diffractogram of $Y_2Ba_4(C_2O_4)_7{\cdot}18H_2O$ precipitated using the segmented flow tubular reactor.

with the 1 μL capillary, a more homogeneous seed population will be prepared, containing more $Y_2Ba_4(C_2O_4)_7{\cdot}18H_2O$ seeds. Increasing the capillary volume makes the mixing conditions less efficient, leading to less homogeneous supersaturation conditions. The seed population would be less homogeneous because seeds other than $Y_2Ba_4(C_2O_4)_7{\cdot}18H_2O$ may be formed. Such a problem should be solved when working with more efficient mixing conditions. The total number of seeds injected in the reactor will also depend on the seed suspension volume. Hence, the total number of seeds eventually present in the reactor will depend on the combination of the seed suspension volume, the reactant rate, and the capillary volume, which is effectively reflected by the important interaction between these factors shown in Figure 6.

These results are difficult to interpret in more depth, as we do not know the precipitation kinetics of these three precipitates. The kinetics should depend on the reactant addition rate, which influences the supersaturation level. Ideally, the addition of the reactant should allow only the growth of the seeds produced from the mixer instead of creating new seeds. With the mixer used in this study, the nucleation conditions are affected. A better control of the nucleation step should take into account the mixer geometry, reactant volume, and flow rate. These concepts were taken into account in the design of a new segmented flow tubular reactor. The tubular reactor uses two nonmiscible phases (aqueous and nonaqueous) to create individual microbatches in which the precipitation reactants are already thoroughly mixed. The noninteracting microvolumes, once segmented in the tubular reactor, will all have the same history, i.e., perfect plug flow regime. This process leads to a more homogeneous reaction than those encountered in larger batch reactors, where poor micromixing can lead to inhomogeneous precipitation products, as experienced in the fed-batch system above. The experimental conditions leading to the precipitation of the higher percentage of the $Y_2Ba_4(C_2O_4)_7{\cdot}18H_2O$ fraction were transferred to our new segmented flow tubular reactor[20] in order to prepare selectively this mixed oxalate.

Segmented Flow Tubular Reactor. The experiment carried out with the tubular reactor was performed at 25 °C to enhance the formation of $Y_2Ba_4(C_2O_4)_7{\cdot}18H_2O$, as seen from the analysis of the 16 batch

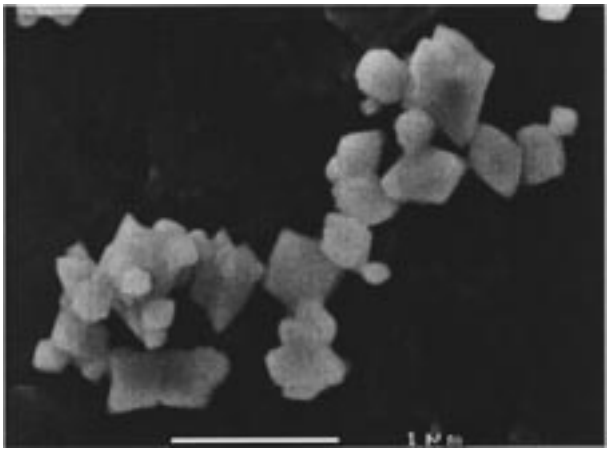

Figure 8. SEM micrograph of octahedral $Y_2Ba_4(C_2O_4)_7 \cdot 18H_2O$ crystals prepared using the segmented flow tubular reactor.

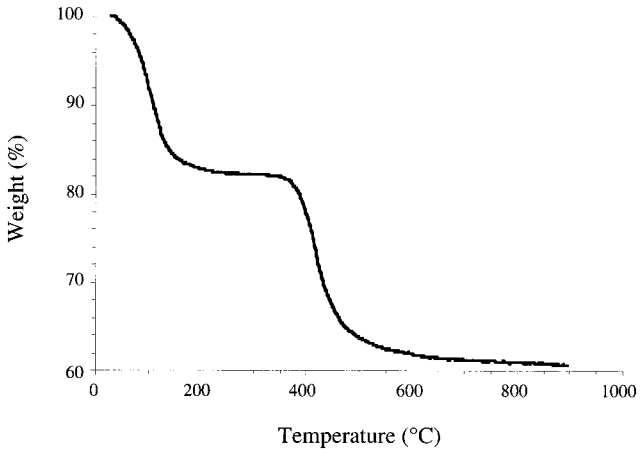

Figure 9. Thermogravimetric analysis of $Y_2Ba_4(C_2O_4)_7 \cdot 18H_2O$.

experiments. The reactants were also less concentrated in order to avoid the nucleation of the other phases.

According to the X-ray diffractogram showed in Figure 7 the powder only contains the mixed phase $Y_2Ba_4(C_2O_4)_7 \cdot 18H_2O$ as the peaks belonging to the other mixed phase do not appear. The micrograph (Figure 8) shows that the powder is composed of octahedral crystals whose size is less than 1 μm. The powder decomposition is achieved in two steps (Figure 9). The first one occurs between 30 and 300 °C (17.81 wt %) and corresponds to the mixed oxalate dehydration, while the second step, which starts at 350 °C and ends by 750 °C (21.2 wt %), corresponds to the decomposition of $Y_2Ba_4(C_2O_4)_7$ into Y_2O_3 and $BaCO_3$. The Ba/Y atomic ratio in the powder is 2.02 ± 0.1. The filtrate composition is $\{Y\} = 1.7 \times 10^{-6}$ M, $\{Ba\} = 3.6 \times 10^{-3}$ M and $\{Oxalate\} = 3.1 \times 10^{-4}$ M. The filtrate pH is 7.04 at 25 °C.

As expected, the tubular reactor improves the selective precipitation of the $Y_2Ba_4(C_2O_4)_7 \cdot 18H_2O$ mixed phase. The Ba/Y atomic ratio of 2.02 confirms that only this phase is precipitated.

4. Conclusions

A new yttrium−barium mixed oxalate forming pinacoidal crystals has been discovered. Its probable composition, $Y_2Ba_2(C_2O_4)_5 \cdot 8H_2O$, has been derived from thermogravimetric data and chemical analysis. The selective synthesis of the mixed oxalate $Y_2Ba_2(C_2O_4)_5 \cdot 8H_2O$ is hoped to be carried out soon to confirm its composition. Assuming the presence of $Y_2Ba_2(C_2O_4)_5 \cdot 8H_2O$, $Y_2Ba_4(C_2O_4)_7 \cdot 18H_2O$, and $BaC_2O_4 \cdot 0.5H_2O$ in a series of precipitates, the effects of precipitation conditions on their relative amounts have been investigated. Statistical analysis of the results shows a good agreement between the weight fractions of $Y_2Ba_4(C_2O_4)_7 \cdot 18H_2O$, as deduced from gravimetric losses and chemical analysis, and the intensity ratios I_1/I_2 of the principal XRD peaks of the different mixed oxalates. Hence, the working hypotheses used to determine the stoichiometry of the new mixed Y−Ba oxalate seem to be reasonably accurate. Statistical analysis of the experimental results shows a complex interplay of the precipitation conditions on the selective formation of the known $Y_2Ba_4(C_2O_4)_7 \cdot 18H_2O$: This mixed oxalate is promoted by low temperature (30 °C), fast addition of reactants, small volume of seed suspension, and small mixing volume. The new mixed oxalate $Y_2Ba_2(C_2O_4)_5 \cdot 8H_2O$ is favored by higher temperature (40 °C), slow reactant addition, high volume of seed suspension, and large mixing volume.

A large part of the complexity of the system seems to originate from the way reactants are mixed prior to their introduction in the reactor, which determines the nucleation step. A better control of nucleation is thus a key issue for controlling the selectivity of mixed oxalate precipitation. To this end, a new segmented flow tubular reactor which permits more homogeneous precipitating conditions has been used to achieve the selective precipitation of $Y_2Ba_4(C_2O_4)_7 \cdot 18H_2O$, leading to a pure phase. This mixed Y−Ba oxalate presents a strong interest in the frame of the preparation of $YBa_2Cu_3O_{7-x}$ superconducting oxides by the oxalate route as it exhibits the same 1−2 stoichiometry for Y and Ba. The knowledge of the solubility constants of both $Y_2Ba_4(C_2O_4)_7 \cdot 18H_2O$ and $Y_2Ba_2(C_2O_4)_5 \cdot 8H_2O$ would be useful to improve the solubility algorithms previously developed[10] and to select more effectively the synthesis conditions of a Y−Ba−Cu oxalate powder for the preparation of $YBa_2Cu_3O_{7-x}$.

Acknowledgment. This work was supported by the Swiss National Fund for Scientific Resarch. N.J. gratefully acknowledges "Stiftung Entwicklungsfonds Seltene Metalle" for a grant. The authors thank Dr. R. Mulone for EDS analysis, Mr. B. Senior for SEM investigations, and Mr. J.-D. Teuscher for the TOC analysis.

CM980745S